

on behalf of
LHeC/FCC-he Study Group

Study of Top Quark FCNC Processes at LHeC and FCC-he: An Attempt to analyse the Lorentz structure of FCNC couplings

30 July, 2021

Based on, Ref: [PRD 100, 015006 (2019), arXiv-2007.02236 S. Behera]

Dr. Subhasish Behera

(Johannes Gutenberg University, Mainz, Germany)

Email: subhparasara@gmail.com, / sbehera@uni-mainz.de

P_L, P_R

γ_μ

$\sigma_{\mu\nu}$

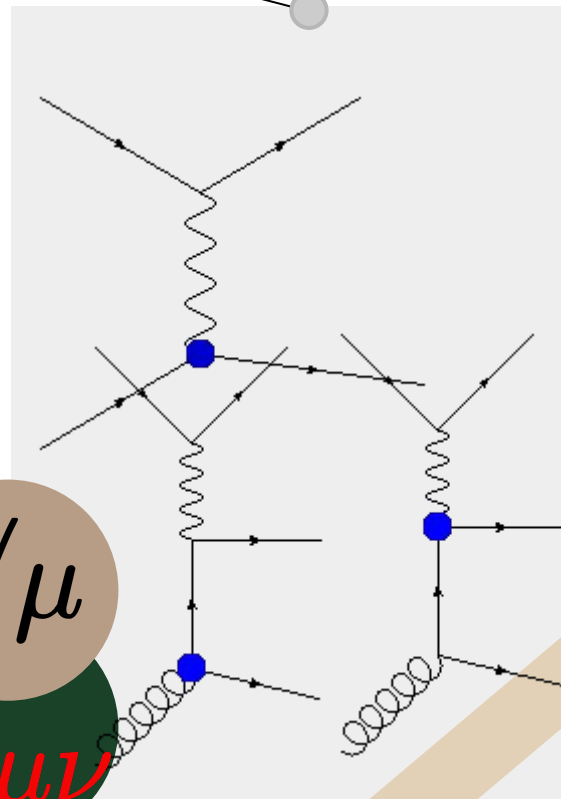




Table of contents

01

Theory I

:EFT Lagrangian, Vector and Tensor couplings

02

Theory II

:Density matrix and Polarization parameters, Asymmetries

03

Simulation & Analysis

:MadGraph5, Pythia6 and Root for Cut Based approach

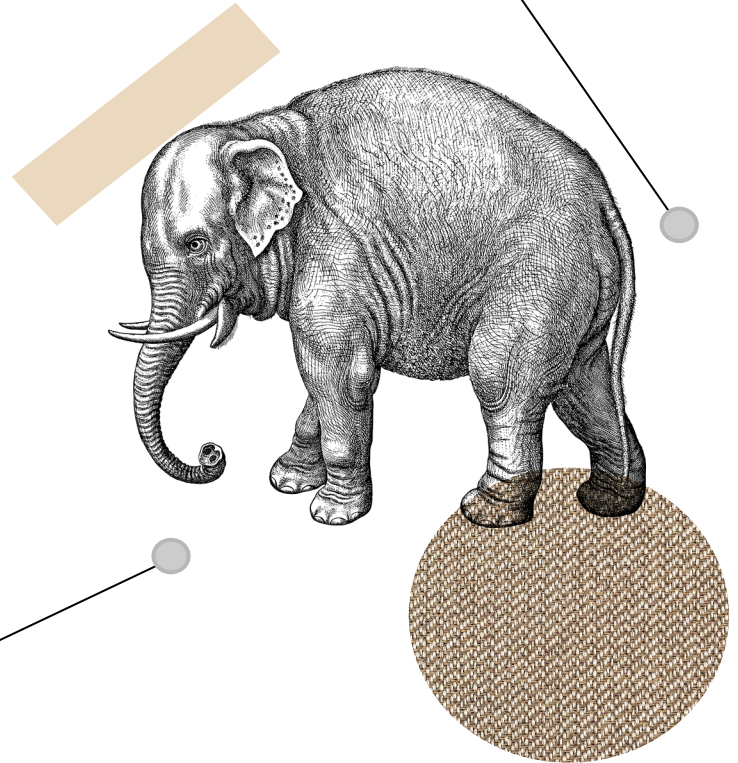
04

Concluding Remarks

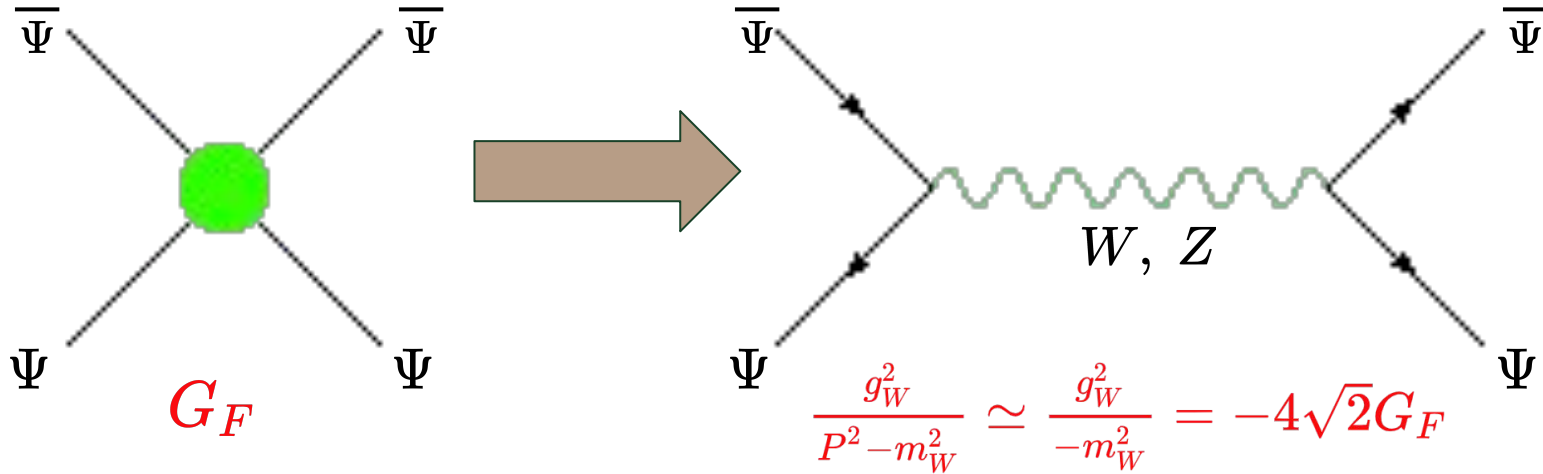
:Results and Motivation

01 Theory I

:EFT Lagrangian, Vector
and Tensor couplings

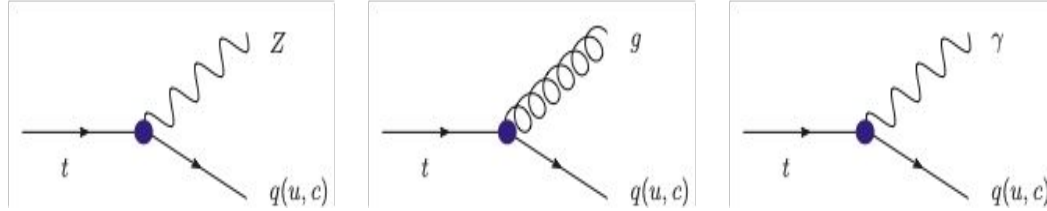


EFT: Why and How?



- If the energy scale of new physics is beyond the reach of recent experiments
- Parameterising lack of information in terms of higher mass dimension operators

Lagrangian for our Study



The complete Effective Lagrangian for top FCNC: [AguilarSaavedra:2008zc]

$$\begin{aligned}
 -\mathcal{L}_{\text{fcnc}} = & g_s \bar{q} \lambda^a \frac{i\sigma^{\mu\nu} q_\nu}{\Lambda} (\kappa_{gqt}^L P_L + \kappa_{gqt}^R P_R) t G_\mu^a \\
 & + e \bar{q} \frac{i\sigma^{\mu\nu} q_\nu}{\Lambda} (\kappa_{\gamma qt}^L P_L + \kappa_{\gamma qt}^R P_R) t A_\mu \\
 & + \frac{g}{2c_W} \bar{q} \gamma^\mu (X_{zqt}^L P_L + X_{zqt}^R P_R) t Z_\mu \\
 & + \frac{g}{2c_W} \bar{q} \frac{i\sigma^{\mu\nu} q_\nu}{\Lambda} (\kappa_{zqt}^L P_L + \kappa_{zqt}^R P_R) t Z_\mu + \text{H.c.},
 \end{aligned}$$

Where, $q(\bar{q}) = u(\bar{u}), c(\bar{c})$ and $q_\nu = (P_t - P_q)$ is the momentum transferred.

FCNC Decay width

$$\Gamma_T(t \rightarrow qg) = \frac{2\alpha_s}{3} |k_{gqt}^{L,R}|^2 \frac{m_t^3}{\Lambda^2},$$

$$\Gamma_T(t \rightarrow q\gamma) = \frac{\alpha}{2} |k_{\gamma qt}^{L,R}|^2 \frac{m_t^3}{\Lambda^2},$$

$$\Gamma_V(t \rightarrow qZ) = \frac{\alpha}{32s_W^2 c_W^2} |X_{zqt}^{L,R}|^2 \frac{m_t^3}{M_Z^2} \left[1 - \frac{M_Z^2}{m_t^2}\right]^2 \left[1 + 2\frac{M_Z^2}{m_t^2}\right],$$

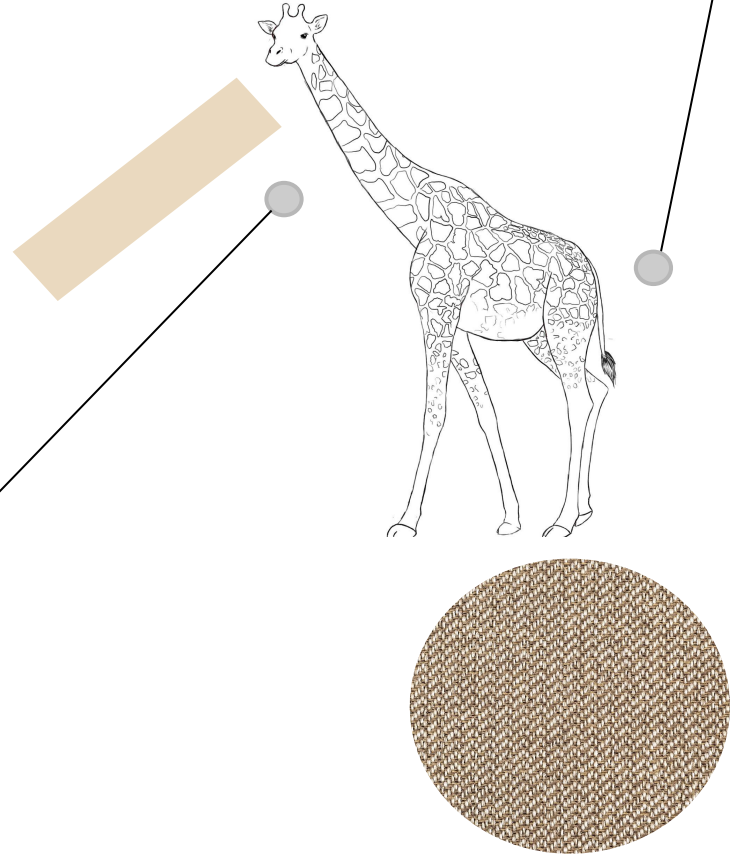
$$\Gamma_T(t \rightarrow qZ) = \frac{\alpha}{16s_W^2 c_W^2} |k_{zqt}^{L,R}|^2 \frac{m_t^3}{\Lambda^2} \left[1 - \frac{M_Z^2}{m_t^2}\right]^2 \left[2 + \frac{M_Z^2}{m_t^2}\right],$$

The subscript (T) and (V) represents the decay width involving either a vector or a tensor coupling, respectively.

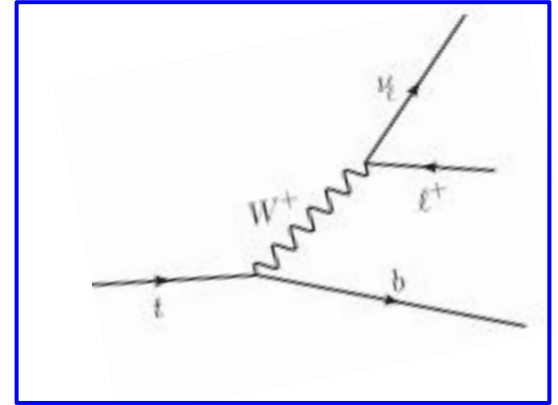
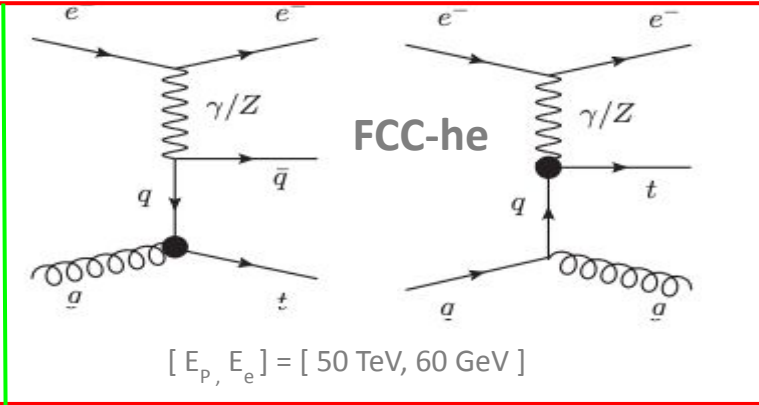
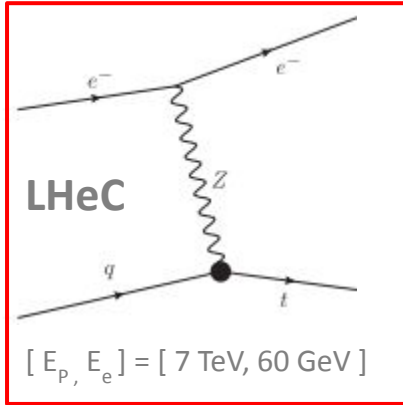
02

Theory II

:Density matrix and
Polarization parameters,
Asymmetries



Density Matrix Formalism



The top quark on-shell condition in the NWA allows one to write the differential cross section of the complete process as:

$$\frac{1}{\sigma_t} \frac{d\sigma_t}{d\Omega_t} = \frac{1}{4\pi} \sum_{\lambda, \lambda'} \sigma(\lambda, \lambda') \mathbf{\Gamma}(\lambda, \lambda')$$

$$\searrow \frac{1}{\sigma_{\text{prod}}} \int \rho(\lambda, \lambda') d\Omega_t,$$

Density Matrix Formalism

Polarization Vector: $\mathbf{P} = (P_x, P_y, P_z)$

The normalized production density matrix elements can be written as:

$$\begin{aligned}\sigma(+, +) &= \frac{1}{2}(1 + P_z) & \sigma(+, -) &= \frac{1}{2}(P_x + iP_y) \\ \sigma(-, -) &= \frac{1}{2}(1 - P_z) & \sigma(-, +) &= \frac{1}{2}(P_x - iP_y)\end{aligned}$$

The normalized decay density matrix elements can be written as:

$$\begin{aligned}\Gamma(+, +) &= \frac{1}{2}(1 + \cos\theta_l) & \Gamma(+, -) &= \frac{1}{2}\sin\theta_l e^{i\phi_l} \\ \Gamma(-, -) &= \frac{1}{2}(1 - \cos\theta_l) & \Gamma(-, +) &= \frac{1}{2}\sin\theta_l e^{-i\phi_l}\end{aligned}$$

Where, θ_l and ϕ_l are the polar and azimuthal angle of the secondary lepton in the **top quark rest frame**.

Polarization Parameters & Spin observables

Observables

$$\frac{1}{\sigma_{\text{tot}}} \frac{d\sigma}{d\Omega_\ell} = \frac{1}{4\pi} \left(1 + P_z \cos \theta_\ell + P_x \sin \theta_\ell \cos \phi_\ell + P_y \sin \theta_\ell \sin \phi_\ell \right)$$

$$A_x \equiv \frac{1}{\sigma_{\text{tot}}} \left[\int_{-\frac{\pi}{2}}^{\frac{\pi}{2}} d\phi_\ell \frac{d\sigma}{d\phi_\ell} - \int_{\frac{\pi}{2}}^{\frac{3\pi}{2}} d\phi_\ell \frac{d\sigma}{d\phi_\ell} \right] = \frac{1}{2} P_x$$
$$A_y \equiv \frac{1}{\sigma_{\text{tot}}} \left[\int_0^\pi d\phi_\ell \frac{d\sigma}{d\phi_\ell} - \int_\pi^{2\pi} d\phi_\ell \frac{d\sigma}{d\phi_\ell} \right] = \frac{1}{2} P_y,$$
$$A_z \equiv \frac{1}{\sigma_{\text{tot}}} \left[\int_0^1 dc_{\theta_\ell} \frac{d\sigma}{dc_{\theta_\ell}} - \int_{-1}^0 dc_{\theta_\ell} \frac{d\sigma}{dc_{\theta_\ell}} \right] = \frac{1}{2} P_z$$

Top quark Rest frame

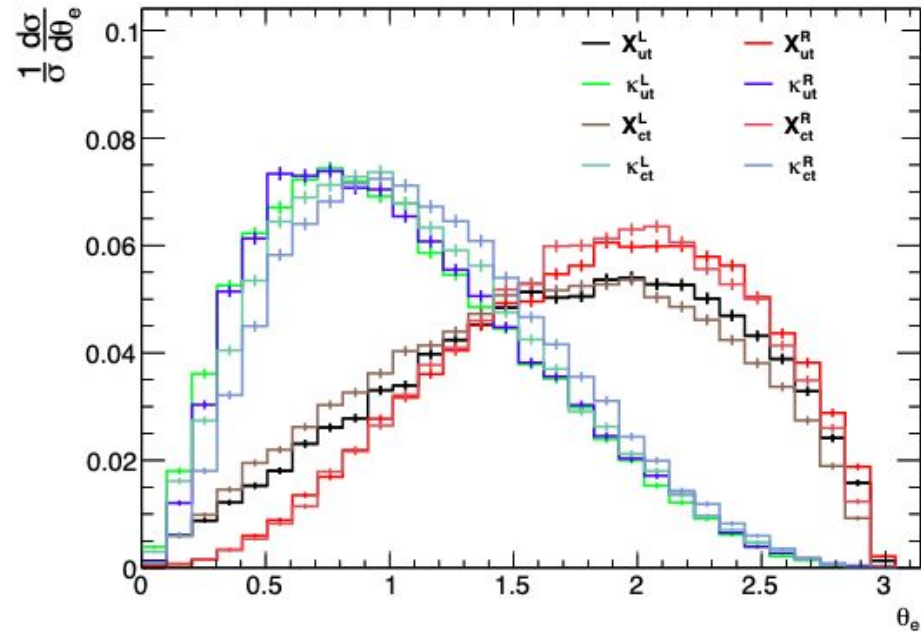
Lab frame of the collider

&

Ref: [PRD 100, 015006 (2019),
arXiv-2007.02236 S. Behera]

$$A_e^{FB} \equiv \frac{\sigma(\cos \theta_e > 0) - \sigma(\cos \theta_e < 0)}{\sigma(\cos \theta_e > 0) + \sigma(\cos \theta_e < 0)}$$

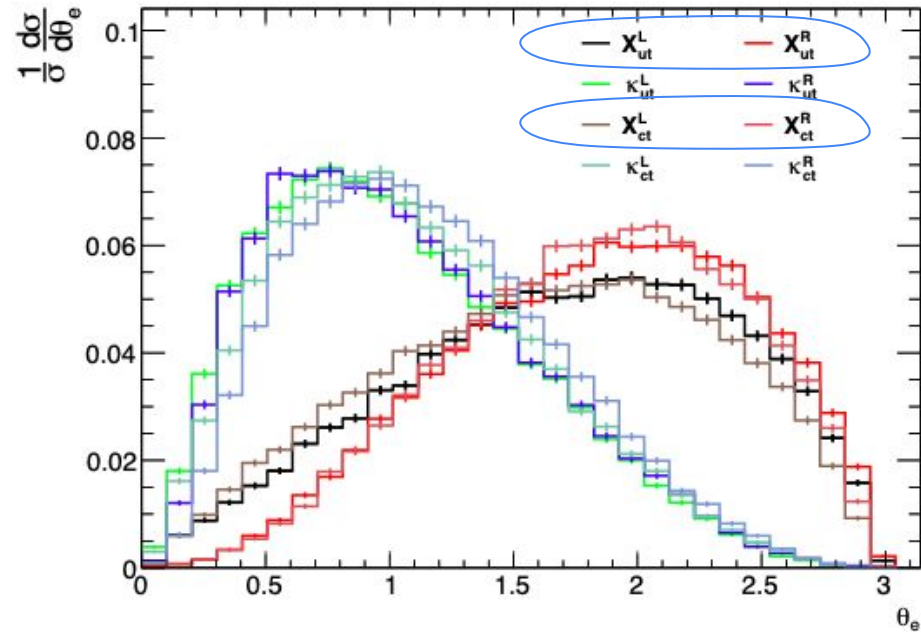
Polarization Parameters & Spin observables



The distributions of polar angle of the scattered electron in the **Lab Frame** of the collider.

→ The Distributions clearly shows the distinction between the vector and tensor couplings.

Polarization Parameters & Spin observables

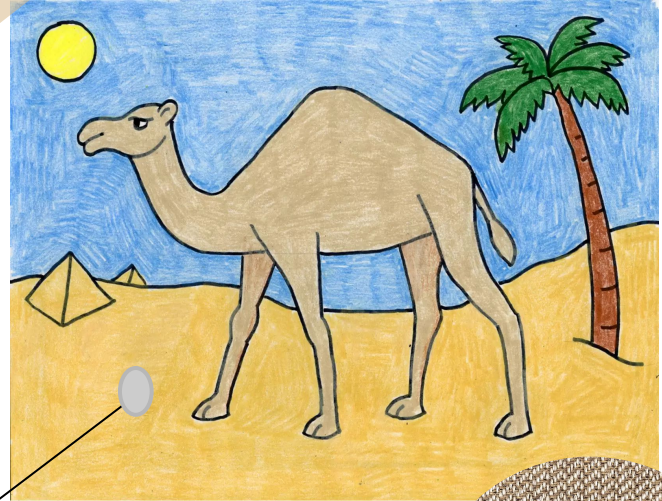


The distributions of polar angle of the scattered electron in the **Lab Frame** of the collider.

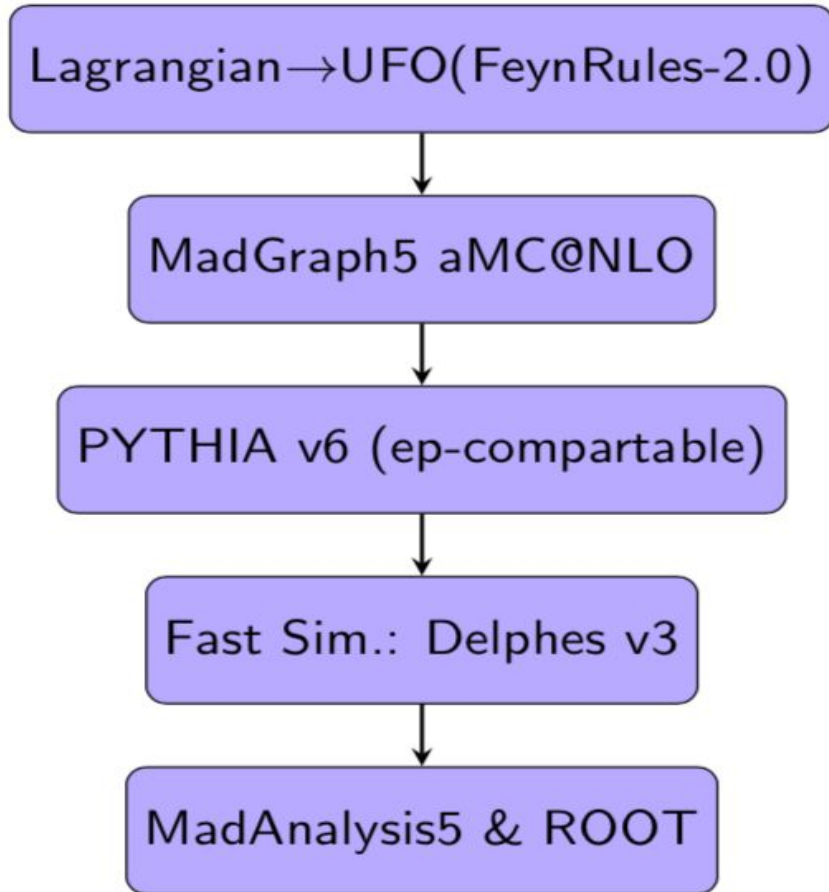
→ The Distributions clearly shows the distinction between the vector and tensor couplings.

03 Simulation & Analysis

:MadGraph5, Pythia6 and
Root for Cut Based
approach



Methodology



- MC setup/Observables
 - PDF set: CTEQ6L1, $\mu_F = \mu_R = m_t$,
 - Preselection: $P_T > 10$ for leptons, jets and $E_T^{\text{Miss}} > 10$ GeV, $|\eta| < 5$. For all jets and leptons
 - Leptons and/or Jets are reconstructed with anti-kT algorithm with cone size of $R = 0.4$
- Selection Cuts [tZq - analysis]
 - $N_{e^-} = N_{e^-, \text{b-jet}} = N_{e^-, \text{b-jet}, l^+} = 1$
- Selection Cuts [tgq & t γ q - analysis]
 - $N_{e^-} = N_{e^-, \text{b-jet}} = N_{e^-, \text{b-jet}, \mu^+/\mu^-} = 1$
 - $N_{\text{Light-jets}} \geq 1$
 - $\Upsilon\mu > 2.6$

CS and Selection Cuts

LHeC

Coupling	Cross section σ in fb for $P_e = -80\%$			
	Basic Cuts	$N_{e^-} = 1$	$N_{e^-,b} = 1$	$N_{e^-,b,\ell^+} = 1$
g_{Ztq}				
X_{ut}^L	1957.57	1763.82	799.65	745.57
X_{ut}^R	1642.47	1485.97	706.09	629.54
κ_{ut}^L	706.77	636.65	304.56	279.13
κ_{ut}^R	1038.68	933.47	474.90	427.77
X_{ct}^L	136.76	122.54	66.90	62.84
X_{ct}^R	103.82	93.05	51.26	47.65
κ_{ct}^L	26.37	23.65	12.96	12.09
κ_{ct}^R	60.00	53.33	29.70	27.45

Bkg processes	$N_{e^-,b,\ell^+} = 1$
Charged Current int.	0.63
Neutral Current int.	0.00
Photo Production int.	1.64

FCC-he

Coupling	κ_{gut}^L	κ_{gut}^R	$\kappa_{\gamma ut}^L$	$\kappa_{\gamma ut}^R$	κ_{gct}^L	κ_{gct}^R	$\kappa_{\gamma ct}^L$	$\kappa_{\gamma ct}^R$	Bkg
$e^-p \rightarrow e^-tj \rightarrow e^-bj\ell^+\nu$ (both e^+ and μ^+ included)									
Basic Cuts	1058.0	1113.2	3198.0	3190.0	498.5	546.2	1420.2	1420.0	485.0
$N_{e^-} = N_{\ell^+} = N_b = 1, N_j \geq 1$	515	550.0	1631.7	1623.2	245.9	271.5	728.1	737.0	8.5
$Y_{\mu^+} > 2.6$	290.1	287.6	530.3	715.8	105.4	82.8	155.9	219.0	0.023
$e^-p \rightarrow e^-tj \rightarrow e^-j\mu^-\nu$									
Basic Cuts	259.4	266.1	831.7	829.1	244.0	248.8	709.4	708.9	485.0
$N_{e^-} = N_{\mu^-} = N_b = 1, N_j \geq 1$	146.4	150.1	467.7	480.1	130.6	128.8	374.1	376.6	4.8
$Y_{\mu^-} > 2.6$	65.8	53.6	102.5	151.0	58.3	47.2	79.6	118.2	0.009

The CS of signal processes are parameterized as follow:

$$\sigma = |g_{vtq}|^2 [\sigma(pe^- \rightarrow e^-t(j)) \times BR(t \rightarrow \ell^+ + b\text{-taggedjet} + MET)]$$

Spin Observables

LHeC

Left-polarized e -beam			
Coupling	A_x	A_z	A_e^{FB}
X^L	-0.16	-0.43	-0.18
κ^L	-0.17	-0.46	+0.63
X^R	+0.07	+0.32	-0.33
κ^R	+0.04	+0.37	+0.65
Right-polarized e -beam			
Coupling	A_x	A_z	A_e^{FB}
X^L	-0.06	-0.43	-0.34
κ^L	-0.01	-0.46	+0.64
X^R	+0.16	+0.32	-0.17
κ^R	+0.16	+0.37	+0.65
Unpolarized e -beam			
Coupling	A_x	A_z	A_e^{FB}
X^L	-0.12	-0.43	-0.24
κ^L	-0.12	-0.46	+0.64
X^R	+0.11	+0.32	-0.26
κ^R	+0.08	+0.36	+0.65

FCC-he

Coupling	No pol.			$P_{e^-} = -80\%$			$P_{e^-} = +80\%$		
	A_x	A_z	$A_{e^-}^{FB}$	A_x	A_z	$A_{e^-}^{FB}$	A_x	A_z	$A_{e^-}^{FB}$
κ_{gut}^L	-0.20	-	-0.22	-0.27	-	-0.28	-0.21	-	-0.20
κ_{gut}^R	0.14	0.40	-0.15	0.16	0.42	-0.23	0.11	0.41	-0.16
$\kappa_{\gamma ut}^L$	-0.33	-0.12	-	-0.31	-0.11	-	-0.30	-0.16	-
$\kappa_{\gamma ut}^R$	-	0.46	-	-	0.47	-	-	0.48	-



Top quark

Coupling	No pol.			$P_{e^-} = -80\%$			$P_{e^-} = +80\%$		
	A_x	A_z	$A_{e^-}^{FB}$	A_x	A_z	$A_{e^-}^{FB}$	A_x	A_z	$A_{e^-}^{FB}$
κ_{gut}^L	-0.35	0.26	-0.48	-0.32	0.28	-0.48	-0.34	0.19	-0.46
κ_{gut}^R	-	0.33	-0.39	-	0.41	-0.47	-	0.32	-0.35
$\kappa_{\gamma ut}^L$	-0.44	-	-0.25	-0.43	-	-0.28	-0.45	-	-0.28
$\kappa_{\gamma ut}^R$	-0.11	0.54	-0.44	-0.14	0.56	-0.37	-	0.53	-0.39



Anti-Top quark

Limits on FCNC couplings

LHeC

FCC-he

$$L = 2 \text{ ab}^{-1}$$

Vector Coupling	Obtainable reach (in part of 10^3)		
	at C.L. = 68%	95%	99%
X_{ut}^L	$\in [-9.8, 9.7]$	$\in [-16.4, 16.4]$	$\in [-20.0, 20.1]$
X_{ut}^R	$\in [-13.7, 13.6]$	$\in [-20.8, 20.9]$	$\in [-24.4, 24.4]$
X_{ct}^L	$\in [-30.8, 31.1]$	$\in [-52.8, 52.7]$	$\in [-65.7, 65.5]$
X_{ct}^R	$\in [-48.0, 47.3]$	$\in [-73.0, 72.7]$	$\in [-85.9, 86.8]$

Tensor Coupling	Obtainable reach (TeV^{-1})		
	at C.L. = 68%	95%	99%
κ_{ut}^L/Λ	$\in [-0.06, 0.06]$	$\in [-0.10, 0.10]$	$\in [-0.13, 0.13]$
κ_{ut}^R/Λ	$\in [-0.07, 0.07]$	$\in [-0.12, 0.12]$	$\in [-0.16, 0.15]$
κ_{ct}^L/Λ	$\in [-0.23, 0.23]$	$\in [-0.40, 0.40]$	$\in [-0.50, 0.50]$
κ_{ct}^R/Λ	$\in [-0.31, 0.31]$	$\in [-0.57, 0.56]$	$\in [-0.71, 0.72]$

Beam polarization	Associated quark	Background events, N_B	Required signal, $N_S(2\sigma)$	Reach of couplings for 95% CL. (TeV^{-1})			
				κ_{qt}^L/Λ	κ_{qt}^R/Λ	$\kappa_{\gamma qt}^L/\Lambda$	$\kappa_{\gamma qt}^R/\Lambda$
Unpolarized	up	46	16	0.029	0.029	0.021	0.019
	charm			0.048	0.054	0.040	0.033
(-80%)	up	34	14	0.028	0.027	0.022	0.017
	charm			0.043	0.037	0.036	0.025
(+80%)	up	28	13	0.030	0.030	0.022	0.019
	charm			0.050	0.056	0.041	0.035

Limits on FCNC couplings

LHeC

$L = 2 \text{ ab}^{-1}$

	BR % ($t \rightarrow Zu$)		BR % ($t \rightarrow Zc$)
$X_{ut}^L = 0.016$	0.009	$X_{ct}^L = 0.053$	0.095
$X_{ut}^R = 0.021$	0.015	$X_{ct}^L = 0.073$	0.181
$\frac{\kappa_{ut}^L}{\Lambda} = 0.10 \text{ TeV}^{-1}$	0.004	$\frac{\kappa_{ct}^L}{\Lambda} = 0.40 \text{ TeV}^{-1}$	0.068
$\frac{\kappa_{ut}^R}{\Lambda} = 0.12 \text{ TeV}^{-1}$	0.006	$\frac{\kappa_{ct}^R}{\Lambda} = 0.57 \text{ TeV}^{-1}$	0.133

FCC-he

$L = 2 \text{ ab}^{-1}$

Coupling	BR $\times 10^5$			
	$t \rightarrow ug$	$t \rightarrow cg$	$t \rightarrow u\gamma$	$t \rightarrow c\gamma$
κ_{Vqt}^L/Λ	1.8	4.3	0.74	1.9
κ_{Vqt}^R/Λ	1.7	3.1	0.44	0.95

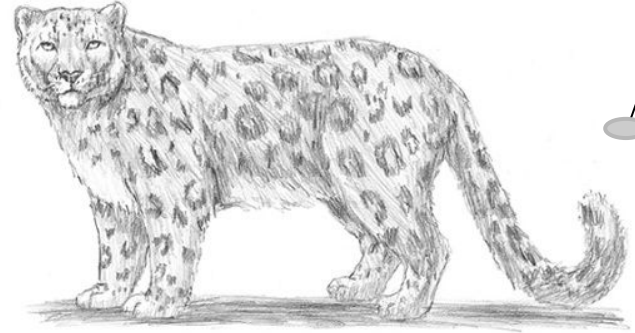
$L = 1 \text{ ab}^{-1}$

	BR % ($t \rightarrow Zu$)		BR % ($t \rightarrow Zc$)
Coupling		Coupling	
$X_{zut}^L = 0.005$	0.051	$X_{zct}^L = 0.013$	0.444
$X_{zut}^R = 0.005$	0.064	$X_{zct}^R = 0.017$	0.754
$\frac{\kappa_{zut}^L}{\Lambda} = 0.035 \text{ TeV}^{-1}$	0.030	$\frac{\kappa_{zct}^L}{\Lambda} = 0.123 \text{ TeV}^{-1}$	0.377
$\frac{\kappa_{zut}^R}{\Lambda} = 0.041 \text{ TeV}^{-1}$	0.043	$\frac{\kappa_{zct}^R}{\Lambda} = 0.172 \text{ TeV}^{-1}$	0.739

LHC

BR limits on 95% C.L.	8/13 TeV	3 ab^{-1} , 14 TeV	15 ab^{-1} , 27 TeV
$t \rightarrow gu$	$4.0(20) \times 10^{-5}$	3.8×10^{-6}	5.6×10^{-7}
$t \rightarrow gc$..	32.1×10^{-6}	10^{-7}
$t \rightarrow Zq$	$1.7(2.4) \times 10^{-4}$	$2.4 - 5.8 \times 10^{-5}$	
$t \rightarrow \gamma u$	0.016(0.182)%	8.6×10^{-6}	
$t \rightarrow \gamma c$..	7.4×10^{-5}	
$t \rightarrow Hq$	-	10^{-4}	

04 Concluding Remarks



Concluding Remarks

- At the LHC, the top quark FCNC are studied mostly by searching for rare decay of the top quark, whereas at LHeC and FCC-he, we can probe these couplings influencing the production itself.
- Study of the vertex structure is very much favourable at the future ep - collider for EW processes in particular
- Only t-channel, EW processes are possible at the production
- Scattered electron from the primary vertex gives extra handle to probe internal structure
- Top quark polarization can be utilized effectively

Summary

Our studies consolidate further the strong case of LHeC/FCC-he for better understanding of the top quark properties and FCNC couplings.

Concluding Remarks

- At the LHC, the top quark FCNC are studied mostly by searching for rare decay of the top quark, whereas at LHeC and FCC-he, we can probe these couplings influencing the production itself.
- Study of the vertex structure is very much favourable at the future ep - collider for EW processes in particular
- Only t-channel, EW processes are possible at the production
- Scattered electron from the primary vertex gives extra handle to probe internal structure
- Top quark polarization can be utilized effectively

Summary

Our studies consolidate further the strong case of LHeC/FCC-he for better understanding of the top quark properties and FCNC couplings.